

Joint Distribution across Representation Space for Out-of-Distribution Detection

Jingwei Xu Siyuan Zhu Zenan Li Chang Xu

State Key Lab of Novel Software Technology, Nanjing University
Nanjing, China

Abstract

Deep neural networks (DNNs) have become a key part of many modern software applications. After training and validating, the DNN is deployed as an irrevocable component and applied in real-world scenarios. Although most DNNs are built meticulously with huge volumes of training data, data in the real world still remain unknown to the DNN model, which leads to the crucial requirement of runtime out-of-distribution (OOD) detection. However, many existing approaches 1) need OOD data for classifier training or parameter tuning, or 2) simply combine the scores of each hidden layer as an ensemble of features for OOD detection. In this paper, we present a novel outlook on in-distribution data in a generative manner, which takes their latent features generated from each hidden layer as a joint distribution across representation spaces. Since only the in-distribution latent features are comprehensively understood in representation space, the internal difference between in-distribution and OOD data can be naturally revealed without the intervention of any OOD data. Specifically, we construct a generative model, called Latent Sequential Gaussian Mixture (LSGM), to depict how the in-distribution latent features are generated in terms of the trace of DNN inference across representation spaces. We first construct the Gaussian Mixture Model (GMM) based on in-distribution latent features for each hidden layer, and then connect GMMs via the transition probabilities of the inference traces. Experimental evaluations on popular benchmark OOD datasets and models validate the superiority of the proposed method over the state-of-the-art methods in OOD detection.

1. Introduction

Deep neural networks (DNNs) receive great achievements in a variety of classification tasks, *e.g.*, image classification, object detection, semantic segmentation, and speech

recognition [1, 11, 12, 23]. Deep learning, as a branch of machine learning, is to build DNN models from the training data, and deploy the well-trained model to the domain that their distributions are assumed the same as the distribution of training data. However, data in real-world is not usually tailored to fit the assumption of identical distribution to the training data, which makes the quality of predictive uncertainty of the DNN models unsure [19]. The predictive uncertainty of DNN models is closely related to the problem of model-specific out-of-distribution (OOD) that distinguishes abnormal samples far away from the distribution of training data [21]. The latter, *i.e.*, detecting OOD data for a given DNN model, is one of the essential requirements when the model prepares for deployment [2].

Hendrycks *et al.* [13] revealed this model-specific OOD detection problem to the society and proposed a baseline method for detection through the softmax value of the target DNN model. In recent years, the primary insight of OOD detection is to design a more effective metric than softmax value to distinguish data from in-distribution to OOD. ODIN [22] applies the temperature scaling [15] to pretrained DNN model to enlarge the gap between in-distribution and OOD data, outperforming popular strategies [28], *e.g.*, MC-Dropout [7], DeepEnsemble [18], and PixelCNN++, [27]. Mahalanobis [21] provides a distance-based approach to attain this goal. They determine the OOD input by computing the Mahalanobis distance between the hidden layer outputs. To improve the detection efficacy, one often preprocesses the input data. For example, ODIN borrows the idea of adversarial attack [9], adding the perturbation to input to separate the in-distribution and OOD data more clearly.

Despite the success of the existing methods [6, 14, 29], they often model the OOD detection problem as a binary classification task and take OOD data as the positive class, which indicates that OOD data is a necessary part in the training phase. In this sense, the proposed OOD detectors actually perform in a discriminative manner [17]. However, the discriminative model for OOD detection can easily be

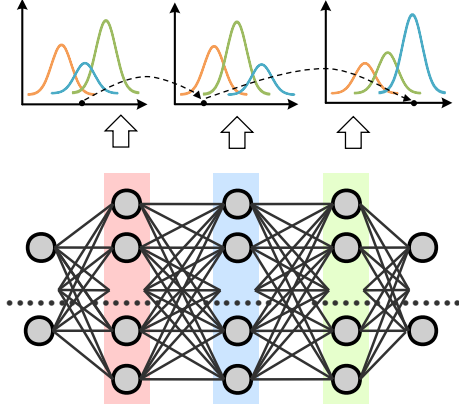


Figure 1. The illustrative example of LSGM. We construct LSGM on the highlighted three hidden layers. For each hidden layer, the distribution is built by Gaussian Mixture model, connected to the distribution of the next layer. Given an input x , the trace of inference across the layers is shown in the figure.

biased to the training OOD dataset, which causes that the other OOD datasets are still mysteries to the model. Contrary to the discriminative model, the generative model is intrinsically able to measure the predictive uncertainty and detect the outliers for the given DNN. The rationale is that the generative model takes OOD detection as a one-class classification task, which is consistent with the general knowledge in classic machine learning [3]. However, outlier detection in classic machine learning is often model-independent due to poor feature extraction for the (statistical) machine learning models. In the era of deep learning, latent features extracted from DNN models could be effective in constructing a generative OOD detector.

In this paper, we construct a DNN model-specific generative model, Latent Sequential Gaussian Mixture (LSGM), to connect the latent features of each representation space in series. LSGM depicts the trace of DNN inference, *i.e.*, recursively generates latent features in one space and transits to the location in the next space. Based on the transitions, the trace of DNN inference across the representation spaces can be revealed as a joint distribution. Thus, we propose a new vision of data distribution from joint spaces rather than one single space. The illustrative example is shown in Fig. 1. As a novel paradigm, LSGM is the first one to explicitly represent the process of input comprehension in the generative manner. Specifically, an input from the in-distribution should obtain a high joint probability on the process of generating the outputs through hidden layers, whereas an OOD input will have a low joint probability (*i.e.*, not similar to the trace of inference for in-distribution data) in the generative model. In addition, as a generative model, LSGM does not need any information from OOD data.

We evaluate the proposed method on three kinds of noise and five real-world benchmark datasets, assuming

OOD datasets are not available for parameter tuning or learning. The experimental results show that the proposed LSGM significantly outperforms state-of-the-art methods, winning 33¹ of 35 cases in evaluation in terms of AUROC.

The main contributions of this paper include:

- A new perspective of model-specific generative model built upon the process of DNN inference, taking the inference trace into a joint distribution.
- A new generative probabilistic graphical model LSGM for to measure the similarity between the trace of DNN inference for the input and the in-distribution data.
- An extensive analysis and evaluation in scenario of learning OOD detector without out-of-distribution data to present the superiority of the proposed LSGM.

The rest of the paper is organized as follows. In Section 2, we present the problem statement and the background. In Section 3, we present our insight, following the description of the proposed LSGM, implementation details, and the relation to Mahalanobis. In Section 4, we present the experimental results. Finally, we conclude the paper in Section 5.

2. Background

2.1. Out-of-Distribution Detection

The OOD detection problem is to identify the abnormal input for a pretrained DNN model. Let $P_{\mathcal{X}}$ be a data distribution defined on input space \mathcal{X} . Let \mathcal{F} represent a DNN model trained on a dataset drawn from the distribution $P_{\mathcal{X}}$. Suppose that there exists one distribution $Q_{\mathcal{X}}$ which is far away from the training distribution $P_{\mathcal{X}}$. In this case, for the DNN model \mathcal{F} , $P_{\mathcal{X}}$ is the in-distribution and $Q_{\mathcal{X}}$ is one of the out-of-distributions. After the deployment of the DNN model \mathcal{F} , we draw a new input x from space \mathcal{X} .

Based on the above notations, we define the following problem:

Problem 1 *The Out-of-Distribution Detection Problem for the pretrained DNN model \mathcal{F}*

Given: An input x drawn from input space \mathcal{X} ,

Find: The probability of that input x is in-distribution.

2.2. Related Work

As discussed in the survey [4], OOD detection falls into the category of unintentional anomaly detection. Given a pretrained DNN model, Hendrycks *et al.* analyzed that the softmax value could statistically distinguish in-distribution

¹Counting without regard to Generalized ODIN, since it must retrain the model, and sacrifice the prediction accuracy (drop about 3% top-1 accuracy) for the detection.

and OOD data [13]. Based on this observation, they used softmax value as a baseline for OOD detection. ODIN [22] improved the baseline with two strategies, *e.g.*, temperature scaling and input preprocessing, to further distinguish in-distribution and OOD data.

Besides softmax, output features of the input in representation spaces could also be leveraged to improve the OOD detector. Some work designed distance-based metrics to distinguish OOD data in representation space. For example, Mahalanobis [21] first takes hidden layers of the DNN model as representation spaces, and then computes Mahalanobis distance to measure how the data belongs to in-distribution in these spaces. Some work involves additional samples to enhance the power of OOD detection during the DNN model training phase. Lee *et al.* aims to train a classifier with a GAN [25, 10] to make the prediction on GAN samples with lower confidence [20]. Outlier Exposure (OE) [14] needs a disjoint OE dataset to mimic the OOD dataset for testing, however the concept of disjoint between OE and OOD is unclear. To detect data from the specific OOD, the above methods all treat the detection as a binary classification problem so that the samples from that OOD are necessities for training the DNN model or the detector.

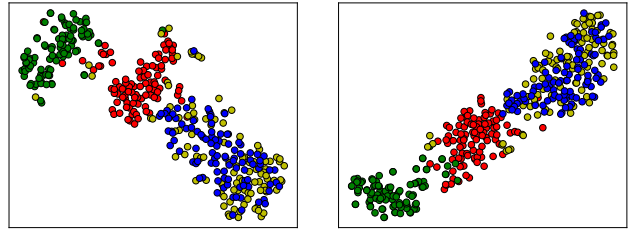
2.3. Gaussian Mixture Model for Latent Feature Generation

When we treat OOD detection as a one-class problem, the proper way is to build a generative model for the detection. Given a model \mathcal{F} , the in-distribution $P_{\mathbf{X}}$, and the target y , a generative model could approximate the probability of $p(\mathbf{x})$, whereas the discriminative model is limited to the estimation of conditional probability $p(y | \mathbf{x})$. As for OOD detection, it is hard to determine $Q_{\mathbf{X}}$ in practice, which makes it impossible for building a proper discriminative model.

Given an input \mathbf{x} , its latent features in representation spaces generated from the hidden layers during DNN inference can also be described by Gaussian Mixture Model, which is a popular generative model. Given a pretrained DNN model and the i -th hidden layer, assume the in-distribution $P_{\mathbf{X}_i}$ on representation space \mathcal{X}_i is formed by clusters, and each cluster is subject to a multivariate Gaussian distribution. Thus, $P_{\mathbf{X}_i}$ could be modeled as a mixture of several multivariate Gaussian distributions, *i.e.*, Gaussian Mixture Model. Suppose the distribution $P_{\mathbf{X}_i}$ has K_i clusters, the marginal distribution of \mathbf{x}_i can be computed by

$$p(\mathbf{x}_i) = \sum_{k=1}^K p(\mathbf{x}_i | z = k)p(z = k),$$

where z is the latent variable with categorical distribution, indicating the probability of the clusters being selected.



(a) Latent features in block1

(b) Latent features in block4

Figure 2. Example of the first observation. Visualizations of latent features are from block1 (randomly selected) and the penultimate layer in ResNet-34 trained on CIFAR-10. In the Figure, in-distribution data (red node) are relatively closed to the center of the representation space.

During the progress of DNN inference, OOD data is often less comprehensively understood in representation spaces, giving a chance to detect OOD data via latent features. Mahalanobis simply combines the distance-based scores in each space in a discriminative way, leaving the relations among the spaces behind. In this paper, we assume a latent feature is generated from a Gaussian Mixture Model on its representation space, and also depend on the latent feature in the previous space. Then, in the view of latent features with series connection, we develop a probabilistic graphical model LSGM to construct the inference trace. Thus, the probability of inference trace estimated by LSGM can be effective in OOD detection.

3. Approach

In this section, we first present the observations of how the deep neural network understands in-distribution data during DNN inference. Then, based on these observations, we design the LSGM, a generative probabilistic graphical model, for latent features generated during the process of DNN inference. We also discuss some implementation details for LSGM, include parameter estimation, Dirichlet Process prior, and fast forward inference. Finally, we illustrate the relations to Mahalanobis, which is a special case of the proposed LSGM.

3.1. Distribution of Latent Features in Representation Space

Feature extraction is one of the intrinsic characteristics of deep neural networks. Given a well pretrained DNN model, the corresponding training set could be comprehensively understood in representation spaces at the hidden layers of the model [8]. We have two observations upon the distribution of latent features to support this assumption.

The first one is *the relatively high centrality of in-distribution data in representation spaces*. Since Batch-Norm is periodically assembled in many DNN models, the latent features should be surrounded in the center of the

corresponding representation space. Taking the ResNet-34 model trained on CIFAR-10 as an example, we randomly select 1,000 samples from in-distribution and three out-of-distribution testing datasets, respectively. Then, we fetch the latent features in a random hidden layer, and visualize the features via t-SNE [24]. As shown in Fig. 2, the in-distribution dataset is clearly separated from other OOD datasets, with relatively centralized in the reduced two-dimensional space.

The second observation is that in-distribution data presents a *smooth distribution of transition between two representation spaces, but the transition from the most OOD data is gathered in few paths*. Since latent features are placed in continuous space, to reveal the transitions across representation spaces, we shall first map these latent features into a discrete space. We build Gaussian Mixture model (GMM) for latent features in the representation space to split these features into clusters. Then, both latent features from in-distribution and OOD testing data are generated by DNN inference, which is the record of the transition paths based on the flows across clusters in two adjacent spaces. Take transitions on ResNet-34 (in-distribution: CIFAR-10 and OOD:SVHN) as an example, the transition distributions from block2 to block3 are visualized in Fig. 3. As shown in Fig. 3(a), the peaks of in-distribution transitions are numerous and low, meaning the data tends to have a smooth distribution across different paths. In contrast, OOD data, which is visualized in Fig. 3(b), concentrates on a few high peaks, demonstrating that OOD data tends to gather in some certain paths. The results from other layers and other DNN models share the same pattern. This phenomenon indicates that the DNN model could comprehensively understand the in-distribution data during inference, whereas they tend to present the one-sided understanding for OOD data. The clear difference from transitions could further demonstrate the effectiveness of the proposed Latent Sequential Gaussian Mixture for OOD detection.

Due to the two observations, we consider the centrality on representation space and discrimination of inference trace, which is a comprehensive understanding for in-distribution data v.s. one-sided understanding for OOD data, could naturally be expert in DNN model-specific OOD detection.

3.2. Latent Sequential Gaussian Mixture

In this part, we present the proposed method LSGM for out-of-distribution detection. The insight of detecting OOD data is to reveal the difference in the trace of DNN inference between in-distribution and OOD data. Since the distributions of latent features from in-distribution data on representation spaces are constructed in DNN training phase, a novel view to the distribution of in-distribution data could be a joint distribution of these latent features on representa-

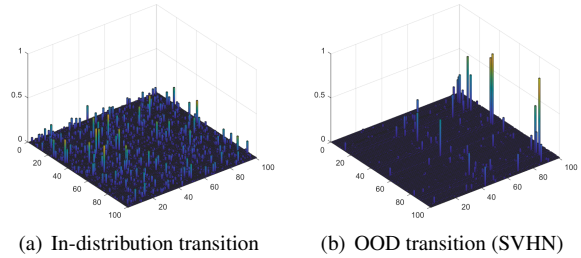


Figure 3. Example of the second observation. Visualization for normalized statistics of transition from block2 to block3 in ResNet-34 trained on CIFAR-10.

tion spaces rather than the distribution on image space.

We construct a generative model that depicts how the latent features are generated in terms of the trace of DNN inference across each representation space. The probabilistic graphical model of LSGM is shown in Fig. 4, and the generative process of LSGM is as follows.

Estimation phase: For each i -th hidden layer,

- Construct GMM_i with a K_i dimensional Categorical distribution Φ_i and a normal distribution Θ_i .
- Estimate parameters Φ_i and Θ_i of GMM_i .
- Estimate the transition matrix $\mathcal{P}_{i,i+1}$.

Inference phase: For an input \mathbf{x} , and denotes its corresponding latent features in i -th layer by \mathbf{x}_i ,

- Compute the mixture weights for each layer:

$$z_i \sim \text{Categorical}(\Phi_i),$$

Let ϕ_{z_i} be mixture weights, *i.e.*, the overall probability of observing a data that comes from i -th component.

- Compute the probability density of latent features \mathbf{x}_i :

$$\mathbf{x}_i \sim \sum_{z_i=1}^{K_i} \phi_{z_i} \mathcal{N}(\mathbf{x} \mid \boldsymbol{\mu}_{z_i}, \boldsymbol{\Sigma}_{z_i}),$$

- Compute the joint probability of inference trace:

$$P(\mathbf{x}_m, \dots, \mathbf{x}_2, \mathbf{x}_1 \mid \Phi, \Theta).$$

Now we focus on how to compute the joint distribution of the latent features $\mathbf{x}_1, \mathbf{x}_2, \dots, \mathbf{x}_m$ across m representation spaces:

$$P(\mathbf{x}_m, \dots, \mathbf{x}_2, \mathbf{x}_1 \mid \Phi, \Theta), \tag{1}$$

where m is the number of hidden layers involved, Φ and Θ are the sets of $\{\Phi_1, \dots, \Phi_m\}$ and $\{\Theta_1, \dots, \Theta_m\}$, respectively. This joint distribution statistically measures the likelihood of these latent features, which are the latent understanding of the DNN model for the given input \mathbf{x} , occurring

together in its trace of DNN inference. Apparently, according to the trace, latent features in representation spaces are not independent. The inference process, in which the current latent features depend on the latent features on previous representation space, is like a chain process. Consider the two connected representation spaces, to generate latent features on later $(i + 1)$ -th representation space, LSGM first decides which component is selected on the previous i -th representation space. Then, the occurrence of the component on later representation space is conditionally based on the previously selected component. After the components are selected on these two representation spaces, latent features are generated based on the component on their own representation space, respectively. Since both z_i and z_{i+1} are categorical variables, a conditional probability table is typically used to represent the conditional distribution.

When we take an observed sequence $\mathbf{x}_1, \mathbf{x}_2, \dots, \mathbf{x}_m$ from DNN inference, all random variables z_1, z_2, \dots, z_m as hidden variables are not specified. Thus, the joint distribution of the sequence is a marginal distribution from the joint distribution of the sequence of $\{\mathbf{x}_1, \dots, \mathbf{x}_m\}$ and all possible traces of $\{z_1, \dots, z_m\}$. Take two observed \mathbf{x}_{i+1} and \mathbf{x}_i as an example, we need to sum up the terms on z_i and z_{i+1} . Notice that two observed \mathbf{x}_{i+1} and \mathbf{x}_i are independent when z_i and z_{i+1} are given specific values. The chain rule of the joint distribution of \mathbf{x}_{i+1} and \mathbf{x}_i is

$$\begin{aligned} &P(\mathbf{x}_{i+1}, \mathbf{x}_i \mid \Phi_i, \Phi_{i+1}) \\ &= \sum_{z_i, z_{i+1}} P(\mathbf{x}_{i+1}, z_{i+1} \mid \mathbf{x}_i, z_i, \Phi_i, \Phi_{i+1}) \\ &= \sum_{k_i, k_{i+1}} P(\mathbf{x}_{i+1} \mid z_{i+1} = k_{i+1})P(\mathbf{x}_i \mid z_i = k_i) \\ &\quad P(z_{i+1} = k_{i+1} \mid z_i = k_i, \Phi_{i+1})P(z_i = k_i \mid \Phi_i). \end{aligned}$$

Since z_i and Φ_{i+1} are independent, the conditional distribution of z_{i+1} given z_i and Φ_{i+1} could be further decomposed as

$$\begin{aligned} &P(\mathbf{x}_{i+1}, \mathbf{x}_i \mid \Phi_i, \Phi_{i+1}) \\ &= \sum_{k_i, k_{i+1}} P(\mathbf{x}_{i+1} \mid z_{i+1} = k_{i+1})P(\mathbf{x}_i \mid z_i = k_i) \\ &\quad P(z_{i+1} = k_{i+1} \mid z_i = k_i) \\ &\quad P(z_{i+1} = k_{i+1} \mid \Phi_{i+1})P(z_i = k_i \mid \Phi_i). \end{aligned} \quad (2)$$

To compute the joint distribution of Eq. (1), the chain rule of the joint distribution could be used for decomposition as follows:

$$\begin{aligned} &P(\mathbf{x}_m, \dots, \mathbf{x}_2, \mathbf{x}_1 \mid \Phi, \Theta) \\ &= \sum_{\mathbf{z}} P(\mathbf{x}_m, z_m \mid \mathbf{x}_{m-1}, z_{m-1}) \\ &\quad \dots P(\mathbf{x}_2, z_2 \mid \mathbf{x}_1, z_1)P(\mathbf{x}_1 \mid z_1)P(z_1), \end{aligned} \quad (3)$$

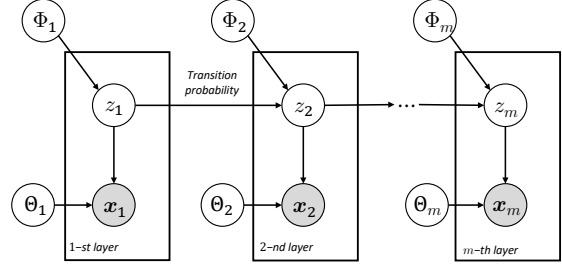


Figure 4. Probabilistic graphical model of LSGM.

where \mathbf{z} is the set of all possible traces $\{z_1, \dots, z_m\}$. Take the decomposed result in Eq. (2), we could expand the above equation in the following:

$$\begin{aligned} &P(\mathbf{x}_m, \dots, \mathbf{x}_2, \mathbf{x}_1 \mid \Phi, \Theta) \\ &= \sum_{\mathbf{z}} P(\mathbf{x}_m, z_m \mid \mathbf{x}_{m-1}, z_{m-1}) \dots P(\mathbf{x}_1 \mid z_1)P(z_1), \\ &= \sum_{\mathbf{z}} \prod_{i=1}^m P(\mathbf{x}_i \mid z_i)P(z_i \mid \Phi_i) \prod_{i=1}^{m-1} P(z_{i+1} \mid z_i). \end{aligned} \quad (4)$$

The joint distribution across representation spaces is the function that measures the degree that the given input \mathbf{x} belongs to the in-distribution data, considering the observations (e.g., latent features) from the trace of DNN inference. By leveraging the multi-spatial latent features, the data distribution is presented as a sequential model across representation spaces, with a Gaussian Mixture Model in each space. The joint distribution is formed during the phase that the DNN model is being trained on the training set, making it proper for the representation of the in-distribution data. OOD data, which is unknown and clearly beyond the cognition of the DNN model, would show great disparity on this joint distribution compared to in-distribution data, making OOD data detected.

3.3. Implementation Details

In this part, we present parameter estimation, fast forward inference, and the Dirichlet Process prior.

Parameter estimation: To use LSGM, the key inferential problem is computing the posterior distribution of the hidden variables given an observed sequence of latent features $\mathbf{x}_1, \mathbf{x}_2, \dots, \mathbf{x}_m$. This distribution is computationally intractable in general. Alternatively, we decompose the parameter estimation in general into several disjoint parts. Each part represents a Gaussian Mixture Model on the corresponding representation space. Since each latent feature \mathbf{x}_i is the observation and only depends on the hidden variable z_i in terms of generative model, the estimation of Φ_i and Θ_i could be solved by classic variational inference. For the transition probabilities in transition matrices, we sta-

tistically count the frequencies from existing traces in in-distribution data as the approximated estimation.

Fast forward inference: Assume m is the number of selected hidden layers and the number of components for each hidden layer is K_i , the time complexity of the forward inference in Eq. (7) is $O(K_i^m)$, which grows exponentially with m . Inspired by the forward algorithm in Hidden Markov Model, we design the following algorithm leveraging the advantage of the conditional independence of LSGM to calculate the probability recursively.

Consider the joint probability $P(z_i, \mathbf{x}_i, \mathbf{x}_{1,\dots,i-1})$ represents the likelihood of z_i and the current observed subsequence $\mathbf{x}_1, \mathbf{x}_2, \dots, \mathbf{x}_{i-1}$. We define the recursive function $\alpha_i(\cdot)$ with the chain rule to expand the joint probability

$$\begin{aligned} \alpha_i(z_i) &= P(z_i, \mathbf{x}_i, \mathbf{x}_{1,\dots,i-1}) \\ &= \sum_{z_{i-1}}^{K_{i-1}} P(z_i, \mathbf{x}_i, z_{i-1}, \mathbf{x}_{1,\dots,i-1}) \\ &= \sum_{z_{i-1}}^{K_{i-1}} P(\mathbf{x}_i | z_i, z_{i-1}, \mathbf{x}_{1,\dots,i-1}) \\ &\quad P(z_i | z_{i-1}, \mathbf{x}_{1,\dots,i-1}) P(z_{i-1}, \mathbf{x}_{i-1}, \mathbf{x}_{1,\dots,i-2}). \end{aligned}$$

In LSGM, \mathbf{x}_i is conditionally independent of other variables except z_i , and z_i is conditionally independent of other variables except z_{i-1} . The above equation could be simplified as follow:

$$\alpha_i(z_i) = P(\mathbf{x}_i | z_i) \sum_{z_{i-1}}^{K_{i-1}} P(z_i | z_{i-1}) \alpha_{i-1}(z_{i-1}).$$

Since $P(\mathbf{x}_i | z_i)$ is given by Gaussian Mixture Model and $P(z_i | z_{i-1})$ is from the transition matrices in LSGM, we could calculate $\alpha_i(z_i)$ from $\alpha_{i-1}(z_{i-1})$ without exponential computation time. Assume K_1, K_2, \dots, K_m have the same value in practice, the time complexity of probability inference with the recursion function is $O(mK_i)$. Since $m \ll K_i$ in practice, the fast forward inference shows linearly w.r.t. the average number of components.

Dirichlet Process prior: The default distribution of latent features on each representation space is approximated via Gaussian Mixture Model. However, Gaussian Mixture Model has several hyperparameters, e.g., number of components, that need manual selection. Consider the infinite number of components, an alternative way is to apply Dirichlet Process prior as a distribution of mixture weights over Gaussian distribution components [26]. Naturally, many of these components will be redundant, and their mixing weights are close to 0, so that we could ignore them from probability mixture. In the implementation, the Dirichlet Process inference uses a truncated distribution with a fixed maximum number of components. Therefore,

the actual number of components used always depends on the data.

3.4. Relations to Mahalanobis

We discuss the generality of LSGM by comparing it to Mahalanobis. Mahalanobis score is calculated as follow:

$$S_{\text{Maha}}(\mathbf{x}) = \sum_i \alpha_i S_{\text{Maha}}^i(\mathbf{x}), \quad (5)$$

where parameter α_i is the weight of the i -th layer, which is learned by using a logistic regression on the OOD data. The $S_{\text{Maha}}^i(\mathbf{x})$ denotes the score of the i -th layer, which is calculated by

$$S_{\text{Maha}}^i(\mathbf{x}) = \max_j -(\mathbf{x}_i - \boldsymbol{\mu}_i^j)^\top \boldsymbol{\Sigma}_i^{-1} (\mathbf{x}_i - \boldsymbol{\mu}_i^j), \quad (6)$$

where the \mathbf{x}_i is the latent feature at the i -th layer, $\boldsymbol{\mu}_i^j$ and $\boldsymbol{\Sigma}_i$ are the j -th class mean and covariance matrix, respectively. The score is calculated via Mahalanobis distance that how the data belongs to the nearest cluster in the selected representation space. Mahalanobis selects a specific trace across representation spaces to execute a weighted summation upon the scores. Consider the score in Eq. (6), assume the class $\boldsymbol{\mu}_i^j$ and covariance matrix $\boldsymbol{\Sigma}_i$ are mean and covariance matrix of a Gaussian distribution on i -th hidden layer, the Mahalanobis score is the log-probability plus a fixed noise. Thus, Mahalanobis could be seen as a special case of LSGM in terms of the specific trace of occurring the nearest cluster on each representation space. By doing this, given an observed sequence of latent features $\mathbf{x}_1, \mathbf{x}_2, \dots, \mathbf{x}_m$, the hidden variables \mathbf{z} are also specified, which makes the trace deterministic instead of probabilistic,

$$\begin{aligned} \text{LSGM}_{\text{Maha}}(\mathbf{x}) &= \log \prod_{i=1}^m P(\mathbf{x}_i | z_i = \text{nearest})^{\alpha_i} \\ &= \sum_{i=1}^m \alpha_i (-\log \sqrt{(2\pi|\boldsymbol{\Sigma}_i|)} - \frac{1}{2} (\mathbf{x}_i - \boldsymbol{\mu}_i^{z_i})^\top \boldsymbol{\Sigma}_i^{-1} (\mathbf{x}_i - \boldsymbol{\mu}_i^{z_i})) \\ &= -\frac{1}{2} \sum_{i=1}^m \alpha_i (\mathbf{x}_i - \boldsymbol{\mu}_i^{z_i})^\top \boldsymbol{\Sigma}_i^{-1} (\mathbf{x}_i - \boldsymbol{\mu}_i^{z_i}) + \epsilon \\ &= -\frac{1}{2} S_{\text{Maha}}(\mathbf{x}) + \epsilon \sim S_{\text{Maha}}(\mathbf{x}) \end{aligned}$$

where α_i is the coefficient for each probability.

4. Experiments

In this section, we demonstrate the effectiveness of the proposed method on several computer vision benchmark datasets. All experiments run on Linux with PyTorch. The code will be released for reproducibility.

Table 1. Detecting in-distribution and OOD test set data for the task of image classification.

Model	In-distribution	OOD	TNR (at 95% TPR)	AUROC	AUPR
Methods: Softmax/ODIN*/Mahalanobis/Mahalanobis*/Generalized ODIN/LSGM					
ResNet	CIFAR-10	Gaussian Noise	76.9/49.7/90.4/99.7/95.8/100	89.7/77.6/97.2/99.9/98.9/100	82.4/65.6/95.8/99.8/98.4/100
		Rademacher Noise	85.6/88.6/97.7/100/99.9/100	93.6/93.8/99.3/100/100/100	87.6/85.3/98.8/100/100/100
		Blob	83.0/56.0/96.8/99.1/96.8/99.8	93.7/80.3/99.4/99.7/99.0/100	90.7/72.2/99.4/99.6/98.4/99.9
		Texture	65.4/42.6/79.9/56.8/82.3/76.4	89.2/79.8/95.2/96.1/91.4/96.2	78.2/65.4/90.3/94.1/88.0/95.0
		LSUN	71.7/56.4/85.9/95.7/84.1/97.0	91.1/81.0/96.6/99.0/96.5/99.3	88.6/71.4/95.8/99.0/96.1/99.3
	iSUN	71.9/56.5/85.5/94.3/83.2/95.9	91.0/81.7/96.3/98.8/96.4/99.0	87.3/70.3/95.0/98.7/95.6/99.0	
	TinyImagenet	71.6/56.6/80.7/94.0/70.4/92.7	91.0/82.4/95.0/98.7/94.2/98.6	88.3/73.3/94.0/98.7/94.1/98.7	
	CIFAR-100	Gaussian Noise	50.7/65.7/57.4/99.6/98.9/100	66.8/85.3/65.1/99.8/99.4/100	54.4/74.8/52.7/99.4/97.7/100
		Rademacher Noise	53.8/85.4/77.2/100/99.8/100	69.8/94.3/88.1/100/99.9/100	56.9/90.0/78.2/100/99.8/100
		Blob	70.1/63.3/78.7/94.7/95.5/98.6	90.0/90.9/90.6/98.4/98.8/99.5	86.5/89.5/84.6/97.4/98.4/98.9
Texture		37.2/21.8/39.5/66.7/70.8/58.5	77.9/77.5/81.2/92.1/92.5/92.9	62.5/67.8/68.4/87.5/86.4/90.7	
LSUN		35.3/35.9/42.0/81.3/77.2/87.0	75.6/84.8/79.0/95.9/93.8/97.0	71.7/85.0/74.1/95.6/91.7/96.6	
iSUN	36.7/36.4/41.6/77.5/75.3/84.4	75.6/85.2/78.5/95.3/93.5/96.5	68.7/83.9/71.0/94.9/90.6/96.0		
TinyImagenet	41.0/45.5/41.6/79.8/77.4/82.1	77.1/87.5/78.9/96.1/94.2/96.4	73.2/87.2/74.5/96.2/92.4/96.5		
DenseNet	CIFAR-10	Gaussian Noise	93.7/96.8/100/100/99.9/100	97.7/98.5/100/100/99.9/100	96.4/95.3/100/100/99.5/100
		Rademacher Noise	93.1/98.0/100/100/99.9/100	97.0/99.0/100/100/100/100	94.1/97.1/100/100/99.9/100
		Blob	0.00/14.1/99.2/98.7/95.8/99.6	64.0/51.2/99.7/99.2/98.2/99.8	56.1/46.7/99.3/97.9/95.2/99.4
		Texture	60.2/8.82/67.6/56.4/82.5/80.8	88.5/68.3/95.2/92.2/96.2/96.8	78.3/58.4/93.9/89.7/93.2/95.6
		LSUN	85.4/80.2/81.1/91.6/95.1/95.7	95.5/93.5/96.4/98.0/98.6/99.0	94.1/89.9/96.6/97.8/97.8/99.0
	iSUN	83.3/77.7/75.2/88.8/94.9/93.0	94.8/92.8/95.6/97.6/98.7/98.6	92.5/88.0/95.5/94.7/96.2/98.6	
	TinyImagenet	81.2/71.1/72.1/89.3/93.7/91.2	94.1/91.3/95.4/97.7/98.4/98.3	92.4/87.6/95.9/97.6/97.8/98.5	
	CIFAR-100	Gaussian Noise	70.8/96.8/100/100/99.8/100	86.6/98.4/100/100/99.9/100	77.8/95.7/100/100/99.5/100
		Rademacher Noise	40.6/85.7/100/100/99.9/100	52.0/91.7/100/100/99.9/100	45.6/81.5/100/100/99.9/100
		Blob	64.0/82.5/96.4/97.2/96.6/99.3	88.0/94.8/98.2/98.4/99.1/99.7	84.7/93.1/94.8/95.3/98.4/98.8
Texture		23.2/19.6/42.0/32.0/62.3/63.8	72.6/73.0/90.0/85.5/90.9/93.6	57.5/57.2/87.7/82.2/85.1/91.4	
LSUN		29.7/38.4/85.4/83.0/89.1/90.6	70.8/79.5/96.7/96.1/97.4/97.7	67.9/75.8/96.2/95.6/96.9/97.5	
iSUN	27.3/35.5/79.0/78.1/87.3/88.0	69.6/78.5/95.9/95.4/97.3/97.3	63.9/72.3/95.5/94.7/96.6/97.0		
TinyImagenet	27.9/36.7/77.0/79.3/89.5/84.7	71.6/80.3/95.8/95.8/97.6/97.1	69.0/77.3/95.9/95.7/97.2/97.2		
WRN	TinyImageNet	Gaussian Noise	49.3/27.2/93.5/94.7/56.1/98.4	63.7/48.0/95.6/96.3/86.6/98.7	52.2/43.9/87.8/88.9/85.0/95.0
		Rademacher Noise	32.1/51.9/98.9/99.6/84.9/99.3	42.4/62.5/99.2/99.7/93.2/99.5	41.5/51.2/97.1/98.7/86.1/97.8
		Blob	38.0/59.8/97.8/98.5/96.0/99.2	66.4/84.6/99.0/99.1/98.7/99.4	56.1/76.8/97.1/97.0/98.0/97.9
		Texture	21.4/18.2/35.8/60.9/39.2/61.8	66.2/72.7/85.2/91.4/83.5/92.4	48.7/61.4/81.1/87.1/76.7/89.1
		LSUN	32.4/34.4/14.0/28.5/26.0/44.2	73.7/75.0/57.0/64.8/67.8/77.4	69.0/69.5/51.6/56.0/62.8/67.8
		iSUN	44.3/55.3/31.2/63.8/34.8/81.5	80.1/86.1/73.8/87.6/74.4/94.2	74.4/82.1/65.1/81.3/69.0/91.3
		CIFAR-10	43.8/74.3/23.0/75.6/56.4/90.8	81.9/94.2/65.3/89.4/89.3/97.0	80.1/93.6/56.9/81.2/88.7/95.0

4.1. Experimental Setup

Networks configurations: In our experiments, we use three popular deep neural networks, ResNet-34, DenseNet-BC ($L=100$, $k=12$, $dropout=0$), and WRN ($L=28$, $widenfactor=2$, $dropout=0.3$) for evaluation. ResNet-34 and WRN are the classic implementations from their original papers [12, 30]. The settings of DenseNet-BC are following the same setup from Mahalanobis².

In-distribution datasets: The experiments involve three in-distribution datasets, CIFAR-10, CIFAR-100, and the large-scale dataset TinyImageNet. The models in experiments were also trained on these datasets.

Out-of-distribution datasets: We choose nine benchmark OOD datasets, including three noises (*e.g.*, Gaussian and Rademacher noises, and Blob) and six real-world datasets (*e.g.*, Texture, LSUN, iSUN, and TinyImageNet).

²https://github.com/pokaxpoka/deep_Mahalanobis_detector

Evaluation metrics: We apply the three most widely used metrics in the previous work to measure the effectiveness of OOD detection. The first one is the true negative rate (TNR) at 95% true positive rate (TPR), which could be interpreted as the probability that an OOD input is correctly identified when the TPR is as high as 95%. The second one is the area under the receiver operating characteristic curve (AUROC) [5]. The AUROC could be interpreted as the model’s ability to discriminate between positive and negative inputs. The third metric is the area under the precision-recall curve (AUPR).

Compared methods: We use five existing methods proposed for OOD detection, *i.e.*, the baseline method [13], ODIN* (without OOD) [22, 16], Mahalanobis (penultimate layer) [21] and its modified version Mahalanobis* (without OOD) [16], and Generalized ODIN (DeConf-C*) [16]. All methods are built without any OOD data.

Hyperparameters: Generative model does not need for

each OOD dataset. We focus on selected layers and the number of components k for building LSGM. In this experiment, we use $k=50$ for models on CIFAR-10, $k=100$ for models on CIFAR-100, and $k=200$ for the model on Tiny-ImageNet in terms of the quantities of classes in datasets. To show the simplicity, we select the last layer of each main block of the model’s architecture for LSGM. No special selection strategy is applied in the evaluation.

4.2. Evaluation Results

4.2.1 Out-of-distribution detection

We evaluate the performance of LSGM compared to other methods built without OOD data. The training data is the training set used for building the DNN model. All test sets of these benchmark datasets are treated as in-distribution and OOD test sets, with 10,000 samples each. To keep the functionality of input preprocessing used in Mahalanobis and ODIN, we adopt a modified input preprocessing strategy, which is introduced in Generalized ODIN. Notice that No input preprocessing is applied for the proposed LSGM. An overall comparison is detailed in Table 1. Mahalanobis and Generalized ODIN both outperform the softmax and ODIN*, and the proposed LSGM is better than them in most cases. The results show strong evidence of the efficacy of OOD detection from generative manner. In particular, our method is the dominant detector for detecting noises, winning 14 of 15 cases in terms of AUROC. Most of the results are 100%, which means a zero error for noise detection.

For OOD real-world datasets, the LSGM outperforms the five compared methods, and is the most stable detector for different OOD data. Note that, Generalized ODIN needs to retrain the DNN model. In evaluation, the top-1 classification accuracies of retrained DNN models drop up to 3.74% according to the difficulty of classification task, which makes it less practical for OOD detection on the DNN models in operation.

Overall, LSGM significantly outperforms these SOTA methods, wining 30 of 35 cases in terms of AUROC, which makes it be a stable method without any assistance of OOD data, showing the good generalization for the detection.

4.2.2 Ablation study

We study the influence of number of components and selected layers for LSGM to the detection performance.

Number of components: Since we apply Gaussian Mixture Model in each representation space, the number of components for Gaussian Mixture Model is one of the key hyperparameters of the proposed LSGM. To analyze the impact of #components to OOD detection, we evaluate multiple LSGMs on ResNet-34 and DenseNet for both CIFAR-10 datasets with different #components settings. Despite the

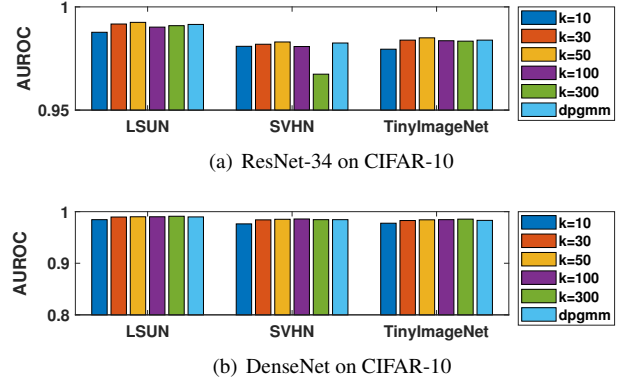


Figure 5. Analysis on the influence on #components for LSGM in representation spaces.

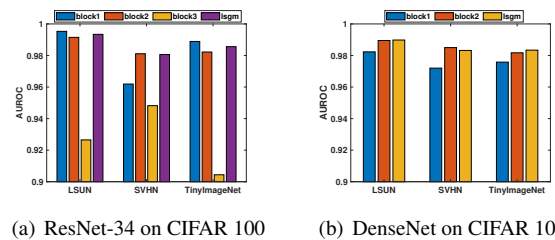
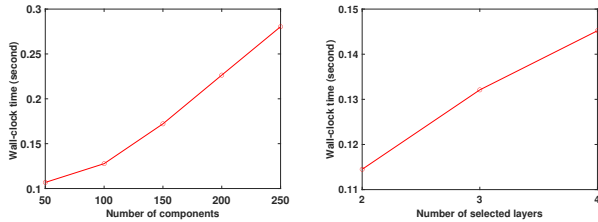


Figure 6. Analysis on the influence on layer selection for LSGM.

manual selection of #components, we also evaluate Dirichlet Process prior as an automated selection approach for #components. The results are shown in Fig. 5. In general, the performance of OOD detection is steady with the increased number of components, with $LSGM_{k=300}$ meeting the highest overall performance in most cases. However, $LSGM_{k=300}$ shows the worst AUROC on SVHN, indicating the lower separability with excessive amount of components for this specific OOD data. Dirichlet Process Gaussian Mixture model (DPGMM) shows the great performance in all cases, which proves the efficacy of searching the true active components in an adaptive manner. As a result, we suggest DPGMM as the default approach to learn the distributions in representation spaces for LSGM.

Impact of layer selection: LSGM consider the inference trace, so the strategy of layer selection is another important thing of the LSGM. To analyze the impact, we also evaluate LSGM on ResNet-34 and DenseNet with three OOD datasets for clarity. We compare the results from Gaussian Mixture Model in each hidden layer and the LSGM, which simply considers all selected layers in series. As the results shown in Fig. 6, it is hard to determine which layer has the best for all OOD data, since the performance of each single layer varies. In contrast, LSGM shows the stable and well performance without the anxiety of layer selection.



(a) Evaluation on different number of components. (b) Evaluation on different number of selected layers.

Figure 7. Time cost evaluation for LSGM applied to WRN model trained on TinyImageNet. The results are average wall-clock time of OOD detection for each input. All numbers of components in hidden layers are the same.

4.2.3 Time cost

In this part, we present the results of the proposed LSGM in terms of efficiency. The experiments are run on a Linux server with two Intel Xeon Gold 5118 CPUs @2.30GHz, 10 GeForce RTX 2080Ti GPUs, and 384GB RAM, running Ubuntu 16.04. In Fig. 7, we show the efficiency of LSGM on WRN model, which is trained on TinyImageNet dataset. The WRN contains four main blocks in the architecture. We follow the strategy of hidden layer selection to uniformly select the last layer in each main block. The number of selected layers is from 2 to 4. We vary number of components K_i in range [50, 250] with the interval 50, while fixing $m = 3$. The sizes of training and testing set are 100, 000 and 10, 000, respectively, and the batch size is 100. The results are the wall-clock time of the whole process of training and testing. As shown in Fig. 7(a) and Fig. 7(b), the proposed LSGM scales linearly when number of components or selected layers increases, respectively.

5. Conclusions

In this paper, we propose a generative probabilistic graphical model across representation spaces, Latent Sequential Gaussian Mixture, to depict the process of DNN inference. The Gaussian Mixture model is used to present the distribution of latent features in each representation space. As a new generative paradigm, LSGM is the first one to explicitly represent the inference via joint spaces in both philosophy and method perspectives. Thus, OOD detection could be solved steadily without the help of any OOD data. Our comprehensive evaluation shows that LSGM is effective and outperforms the compared methods.

References

[1] T. Afouras, J. S. Chung, A. Senior, O. Vinyals, and A. Zisserman. Deep audio-visual speech recognition. *IEEE Transactions on Pattern Analysis and Machine Intelligence*, pages 1–1, 2018. 1

[2] Dario Amodei, Chris Olah, Jacob Steinhardt, Paul Christiano, John Schulman, and Dan Mané. Concrete problems in ai safety. *arXiv preprint arXiv:1606.06565*, 2016. 1

[3] Irad Ben-Gal. Outlier detection. In *Data mining and knowledge discovery handbook*, pages 131–146. Springer, 2005. 2

[4] Saikiran Bulusu, Bhavya Kailkhura, Bo Li, Pramod K. Varshney, and Dawn Song. Anomalous example detection in deep learning: A survey, 2021. 2

[5] Jesse Davis and Mark Goadrich. The relationship between precision-recall and roc curves. In *Proceedings of the 23rd international conference on Machine learning*, pages 233–240, 2006. 7

[6] Akshay Raj Dhamija, Manuel Günther, and Terrance E. Boult. Reducing network agnostophobia. In *Proceedings of the 32nd International Conference on Neural Information Processing Systems*, NIPS’18, pages 9175–9186, 2018. 1

[7] Yarin Gal and Zoubin Ghahramani. Dropout as a bayesian approximation: Representing model uncertainty in deep learning. In *International conference on machine learning*, pages 1050–1059, 2016. 1

[8] Ian Goodfellow, Yoshua Bengio, Aaron Courville, and Yoshua Bengio. *Deep learning*, volume 1. MIT press Cambridge, 2016. 3

[9] Ian Goodfellow, Jonathon Shlens, and Christian Szegedy. Explaining and harnessing adversarial examples. In *International Conference on Learning Representations*, 2015. 1

[10] Ian J. Goodfellow, Jean Pouget-Abadie, Mehdi Mirza, Bing Xu, David Warde-Farley, Sherjil Ozair, Aaron Courville, and Yoshua Bengio. Generative adversarial networks. *Advances in Neural Information Processing Systems*, 3:2672–2680, 2014. 3

[11] Kaiming He, Georgia Gkioxari, Piotr Dollár, and Ross Girshick. Mask r-cnn. In *Proceedings of the IEEE international conference on computer vision*, pages 2961–2969, 2017. 1

[12] Kaiming He, Xiangyu Zhang, Shaoqing Ren, and Jian Sun. Deep residual learning for image recognition. In *Proceedings of the IEEE conference on computer vision and pattern recognition*, pages 770–778, 2016. 1, 7

[13] Dan Hendrycks and Kevin Gimpel. A baseline for detecting misclassified and out-of-distribution examples in neural networks. In *International Conference on Learning Representations (ICLR)*, 2017. 1, 3, 7

[14] Dan Hendrycks, Mantas Mazeika, and Thomas Dietterich. Deep anomaly detection with outlier exposure. 2019. 1, 3

[15] Geoffrey Hinton, Oriol Vinyals, and Jeff Dean. Distilling the knowledge in a neural network, 2015. 1

[16] Yen-Chang Hsu, Yilin Shen, Hongxia Jin, and Zsolt Kira. Generalized odin: Detecting out-of-distribution image without learning from out-of-distribution data. In *Proceedings of the IEEE/CVF Conference on Computer Vision and Pattern Recognition*, pages 10951–10960, 2020. 7

[17] Tony Jebara. *Machine learning: discriminative and generative*, volume 755. Springer Science & Business Media, 2012. 1

[18] Balaji Lakshminarayanan, Alexander Pritzel, and Charles Blundell. Simple and scalable predictive uncertainty estimation using deep ensembles. In *Advances in Neural Information Processing Systems*, pages 6402–6413, 2017. 1

- [19] Kimin Lee, Honglak Lee, Kibok Lee, and Jinwoo Shin. Training confidence-calibrated classifiers for detecting out-of-distribution samples. *arXiv preprint arXiv:1711.09325*, 2017. [1](#)
- [20] Kimin Lee, Honglak Lee, Kibok Lee, and Jinwoo Shin. Training confidence-calibrated classifiers for detecting out-of-distribution samples. In *International Conference on Learning Representations*, 2018. [3](#)
- [21] Kimin Lee, Kibok Lee, Honglak Lee, and Jinwoo Shin. A simple unified framework for detecting out-of-distribution samples and adversarial attacks. In *Advances in Neural Information Processing Systems*, pages 7167–7177, 2018. [1](#), [3](#), [7](#)
- [22] Shiyu Liang, Yixuan Li, and Rayadurgam Srikant. Enhancing the reliability of out-of-distribution image detection in neural networks. In *International Conference on Learning Representations (ICLR)*, 2018. [1](#), [3](#), [7](#)
- [23] Jonathan Long, Evan Shelhamer, and Trevor Darrell. Fully convolutional networks for semantic segmentation. In *Proceedings of the IEEE conference on computer vision and pattern recognition*, pages 3431–3440, 2015. [1](#)
- [24] Laurens van der Maaten and Geoffrey Hinton. Visualizing data using t-sne. *Journal of machine learning research*, 9(Nov):2579–2605, 2008. [4](#)
- [25] Alec Radford, Luke Metz, and Soumith Chintala. Unsupervised representation learning with deep convolutional generative adversarial networks. In *International Conference on Machine Learning*, 2016. [3](#)
- [26] Carl Edward Rasmussen. The infinite gaussian mixture model. In *Proceedings of the 12th International Conference on Neural Information Processing Systems, NIPS'99*, pages 554–560, Cambridge, MA, USA, 1999. MIT Press. [6](#)
- [27] Tim Salimans, Andrej Karpathy, Xi Chen, and Diederik P. Kingma. Pixelcnn++: Improving the pixelcnn with discretized logistic mixture likelihood and other modifications. In *International Conference on Learning Representations*, 2017. [1](#)
- [28] Alireza Shafaei, Mark Schmidt, and James J. Little. A less biased evaluation of out-of-distribution sample detectors. 2019. [1](#)
- [29] Apoorv Vyas, Nataraj Jammalamadaka, Xia Zhu, Dipankar Das, Bharat Kaul, and Theodore L. Willke. Out-of-distribution detection using an ensemble of self supervised leave-out classifiers. In *In Proceedings of the European Conference on Computer Vision*, 2018. [1](#)
- [30] Sergey Zagoruyko and Nikos Komodakis. Wide residual networks. In *BMVC*, 2016. [7](#)